Simulation of Stochastic Loads for Fatigue Experiments

Sørensen, John Dalsgaard; Brincker, Rune

Publication date:
1987

Document Version
Publisher's PDF, also known as Version of record

INSTITUTTET FOR BYGNINGSTEKNIK
INSTITUTE OF BUILDING TECHNOLOGY AND STRUCTURAL ENGINEERING
AALBORG UNIVERSITETSCENTER · AUC · AALBORG · DANMARK

STRUCTURAL RELIABILITY THEORY
PAPER NO. 31

J. D. SØRENSEN & RUNE BRINCKER
SIMULATION OF STOCHASTIC LOADS FOR FATIGUE EXPERIMENTS

NOVEMBER 1987
ISSN 0902-7513 R8717

The STRUCTURAL RELIABILITY THEORY papers are issued for early dissemination of research results from the Structural Reliability Group at the Institute of Building Technology and Structural Engineering, University of Aalborg. These papers are generally submitted to scientific meetings, conferences or journals and should therefore not be widely distributed. Whenever possible reference should be given to the final publications (proceedings, journals, etc.) and not to the Structural Reliability Theory papers.

INSTITUTTET FOR BYGNINGSTEKNIK

INSTITUTE OF BUILDING TECHNOLOGY AND STRUCTURAL ENGINEERING

AALBORG UNIVERSITETSCENTER · AUC · AALBORG · DANMARK

STRUCTURAL RELIABILITY THEORY

PAPER NO. 31

J. D. SØRENSEN & RUNE BRINCKER

SIMULATION OF STOCHASTIC LOADS FOR FATIGUE EXPERIMENTS

NOVEMBER 1987 ISSN 0902-7513 R8717

Simulation of Stochastic Loads for Fatigue Experiments

John Dalsgaard Sørensen & Rune Brincker
University of Aalborg
Sohngaardsholmsvej 57, DK-9000 Aalborg
Denmark

ABSTRACT

A simple direct simulation method for stochastic fatigue load generation is described in this paper. The simulation method is based on the assumption that only the peaks of the load process significantly affect the fatigue life. The method requires the conditional distribution functions of load ranges given the last peak values. Analytical estimates of these distribution functions are presented in the paper and compared with estimates based on a more accurate simulation method. In the more accurate simulation method samples at equidistant times are generated by approximating the stochastic load process by a Markov process. Two different spectra from two tubular joints in an offshore structure (one narrow banded and one wide banded) are considered in an example. The results show that the simple direct method is quite efficient and is results in a simulation speed at about 3000 load cycles per second using an IBM PC. Finally the proposed simulation method for fatigue load generation is tested by comparing some fatigue damage measures obtained by the simulation methods.

1 INTRODUCTION

For structural systems where the fatigue failure mode is of importance it is generally necessary to model the load on the structure as a stochastic process in order to give a realistic description of the load. For example structures such as slender bridges, towers and offshore structures subjected to wind, sea waves or earthquakes are exposed to loads of distinct stochastic nature. In this paper we assume the load to be modelled by stationary stochastic processes although it is quite seldom to expect real loads to remain stationary during the whole lifetime of a structure. However, some quasi-stationary periods can usually be distinguished.

Besides the stochastic load also stochastic material properties have influence on the lifetime of the so-called fatigue failure elements (potential fatigue failure areas). In the last decade there has been significant progress in the theoretical description of stochastic fa-

tigue processes based on fracture mechanics, see e.g. Madsen[1] and Sobczyk[2]. However, in order to use these models in practical problems it is necessary to perform experiments to get information about the material properties. These experiments have to be performed with stochastic load contrary to experiments up till now, which have almost all been performed with cyclic deterministic loads. Further, in order to study the fatigue process under stochastic load in general it is desirable to be able to perform experiments with stochastic loading.

In this paper the problem of simulating stochastic loads for experimental investigations is considered. In Brincker & Sørensen[3] another but related problem is considered, namely the experimental problem of exposing a test specimen to the simulated load history. Assuming that we are not dealing with rate sensitive problems (corrosion, creep, etc.) the problem is here to be able to apply the loads quickly enough to finish the test within a reasonable time (as fast as possible) being sure that the errors introduced by the load equipment do not significantly influence the test results. Results shown in ref. 3 indicate that using a simple computer based control principle and the simple direct simulation method described in this paper it is possible to perform fatigue experiments with simultaneous simulation at speeds up to about 150 load cycles per second without introducing any errors of significance.

Two simulation methods are described in detail in this paper. The first and most accurate method is based on simulation of samples at equidistant times by approximating the stochastic load process by a Markov process. Simulation of a load realization by this method is relatively slow compared with the other simple direct method which is based on the assumption that only the peaks of the load process significantly affect the fatigue life. This simple direct method requires the conditional distribution functions of load ranges given the last peak values. Analytical approximations of these distribution functions are presented in the paper. The approximation introduced is that the first passage density function of the time between successive extremes of the load process is approximated by the density function of the time between zero crossings of the derivative process. The analytical estimates are compared with simulation results based on the more accurate simulation method for two different spectra from two tubular joints in an offshore structure (one narrow banded spectrum and one wide banded spectrum). Finally, the proposed simulation method for fatigue load generation is tested by comparing some fatigue damage measures obtained by the two simulation methods.

2 DIRECT SIMULATION OF STOCHASTIC LOADS FOR FATIGUE EXPERIMENTS

Realizations of stochastic processes can be simulated in a number of different ways. In this paper we consider a stochastic process $\{Z(t), t \in T^*\}$, where T^* is the time index set. The process is assumed to be stationary and Gaussian with zero mean, unit standard deviation and a two-sided spectral density function $S_Z(\omega)$, where ω is the cyclic frequency.

If the spectrum is approximated by a Fourier amplitude spectrum, realizations of the

process can be generated by weighting a superposition of a large number of sinusoids at equispaced frequencies with randomly generated phase angles, Borgman[4] and Yang[5]. Another class of simulation methods which uses models formulated explicitly in discrete time is the autoregressive/moving average (ARMA) models. These models can be represented as stochastic linear difference equations of finite order, Box & Jenkins[6], Chang et al[7] and Krenk & Clausen[8]. Closely related to ARMA models are methods formulated in continuous time, where realizations are generated at equidistant times, see e.g. Franklin[9,10]. These methods generate outcomes of models which can be represented by stochastic differential equations of finite order, see section 3.

In order to reduce the total time for a fatigue experiment it is important to be able to simulate the stochastic load very quickly. If the spectrum has to be represented accurately the methods based on superposition of sinusoids generally require a large number of sinuoids. Therefore, it is not relevant generally to use these methods to generate stochastic fatigue loads when compared with the other methods mentioned above which are based on approximations of the load spectra by rational spectra of usually low order and only require relatively simple calculations to generate the realizations.

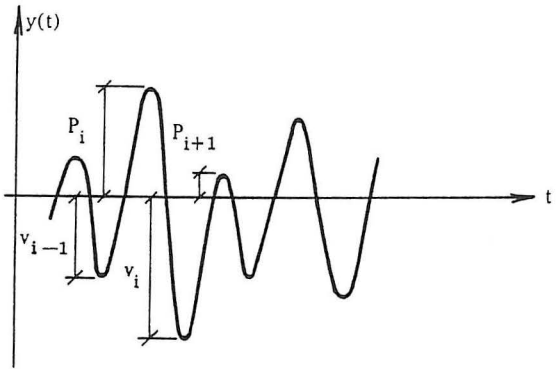

Figure 1. Realization of load process.

The above methods all generate realizations at equidistant times. However, most models of fatigue damage assume that the fatigue load can be represented by the ranges between successive extremes of the load process, see figure 1. In this paper it is described how fatigue loads can be generated by direct simulation of the extremes only. By this method a relatively coarse approximation $\{Y(t)\}$ to $\{Z(t)\}$ is generated, but examples indicate that the fatigue damage measures estimated from realizations by this method are only sligthly different from measures obtained by using the more accurate simulation method based on solving linear differential equations. As described in ref. 3 a simulation method which only generates outcomes of the extremes of a stochastic process is easily incorporated in an adaptive control system for experimental tests.

Let v_i and p_i denote the values of the valley and the peak in the ith load cycle. v_i and p_i are generated from

$$v_i = p_i - e_i^p(p_i) \tag{1}$$

$$p_i = v_{i-1} + e_i^v(v_{i-1}) \tag{2}$$

where $e_i^p(p_i)$ and $e_i^v(v_{i-1})$ are realizations of conditional stochastic variables $E^p(p)$ and $E^v(v)$ modelling the range between successive extremes given the preceding peak or valley. By this approximation the influence of time is neglected. Simulation of $e_i^p(p_i)$ and $e_i^v(v_{i-1})$ requires information about the conditional distribution of ranges given the preceding extreme. This information can be obtained by analytical estimates of the conditional distribution functions or by simulation. In the following two sections it is shown how the simulation and the analytical estimates can be obtained.

(1) and (2) can be considered as a Markov approximation of the stochastic process defined by the extremes of $\{Z(t)\}$. A further simplification is obtained if the dependence of the previous extreme is neglected in the model. In this case only the distribution of ranges is needed. On the other hand better approximations can be obtained if the ranges in (1) and (2) are conditioned on more than just the previous extreme.

Due to symmetry of $\{Z(t)\}$ $E^p(p)$ and $E^v(v)$ can be modelled by a single stochastic variable $E(y)$. Realizations of $E(y)$ can be obtained using an inverse technique where realizations of independent stochastic variables uniformly distributed between 0 and 1 and the conditional distribution function of E given y are used. Realizations of independent and uniformly distributed variables can be generated by e.g. the pseudo-random generators of the mixed-congruential type, see Hammersley[11].

A practical implementation of the above method requires a discretization of the sample space of the stochastic process. Let $[-x_a, x_a]$ be the interval of interest. If this interval is divided into N subintervals simulation of realizations of the extremes by the above method requires estimation of a $N \times N$ matrix with elements specifying the conditional probability of a given range given an extreme. Based on this probability matrix a so-called jump matrix can be constructed. The i,j th element in this matrix gives the jump e_{ij} to the next extreme given that the latest extreme was $x_a(j\frac{2}{N} - 1)$ (a valley) or $x_a(1 - j\frac{2}{N})$ (a peak) and that the generated pseudo-random number is in the interval $[\frac{i-1}{N}, \frac{i}{N}]$. It is assumed that $e_{ij} \in \{k\frac{2x_a}{N} \quad , k = 0, 1, 2, \cdots, N-1\}$.

3 CONTINUOUS SIMULATION BY MARKOV APPROXIMATION USING CONSTANT TIME STEP

In this section a simulation method is described which can be used to estimate the jump matrix used in the simple direct simulation method and to evaluate the accuracy of the simple simulation method. The method, see Franklin[9,10] can be used to simulate realizations of a normal stationary stochastic process by approximating the stochastic process $\{Z(t)\}$ by a normal Markov process $\{X(t)\}$ which is characterized by the assumption that its spectral density can be written as

$$S_X(\omega) = \frac{1}{2\pi}\left|\frac{P(i\omega)}{Q(i\omega)}\right|^2 \tag{3}$$

where

$$P(i\omega) = p_0(i\omega)^m + p_1(i\omega)^{m-1} + \cdots + p_{m-1}(i\omega) + p_m \tag{4}$$

$$Q(i\omega) = (i\omega)^n + q_1(i\omega)^{n-1} + \cdots + q_{n-1}(i\omega) + q_n \tag{5}$$

S_X is assumed to be integrable which implies $n > m \geq 0$. Further the zeroes of Q have to fulfil $Re(i\omega) < 0$. From (3) it is seen that $\{X(t)\}$ can be obtained as the output from a linear system with frequency response function $\frac{P(i\omega)}{Q(i\omega)}$ loaded by a white noise process $\{F(t)\}$. The differential equations corresponding to this system can be written

$$X(t) = P(\frac{d}{dt})\Gamma(t) \tag{6}$$

$$Q(\frac{d}{dt})\Gamma(t) = F(t) \tag{7}$$

If realizations of $\Gamma(t)$, $\frac{d}{dt}\Gamma(t), \cdots, \frac{d^m}{dt^m}\Gamma(t)$ are known, realizations of $X(t)$can be determined by (6). In Franklin[9,10] it is shown that realizations of the vector

$$\overline{\Gamma}(t) = \begin{pmatrix} \Gamma(t) \\ \Gamma^1(t) \\ \vdots \\ \Gamma^{n-1}(t) \end{pmatrix} \tag{8}$$

can be obtained incrementally from

$$\overline{\Gamma}(t + \Delta t) = \overline{\overline{U}}(\Delta t)\overline{\Gamma}(t) + \overline{\overline{T}}\,\overline{W} \tag{9}$$

$\Gamma^j(t)$ denotes the jth derivative of $\Gamma(t)$. $\overline{\overline{U}}(\Delta t)$ and $\overline{\overline{T}}$ are matrices with elements depending on Δt and $q_1, q_2, \cdots, q_n$,see Franklin[9,10]. $\overline{W}$ is an n-dimensional vector of independent and normally distributed variables with mean zero and standard deviation one.

Given a spectrum $S_Z(\omega)$ an approximation $S_X(\omega)$ of the form (3) can be obtained by assuming n equal and solving a curve fitting problem where the optimization variables $x_1, x_2, \cdots, x_{n+m+1}$ are connected to $\overline{p}$ and $\overline{q}$ as follows

$$p_j = x_{n+1+j} \quad , j = 0, 1, \cdots, m \tag{10}$$

$$q_j = (-1)^j \sum_{k_1 < k_2 < \cdots < k_j} \prod_{l=1}^{j} (i\omega_{k_l}) \quad , j = 1, 2, \cdots, n \tag{11}$$

where ($*$ denotes complex conjugate)

$$\begin{aligned} \omega_1 &= x_1 + ix_2 \\ \omega_2 &= -x_1 + ix_2 \\ &\vdots \\ \omega_{n-1} &= x_{n-1} + ix_n \\ \omega_n &= -x_{n-1} + ix_n \\ \omega_{n+j} &= \omega_j^* \end{aligned} \tag{12}$$

The curvefitting problem is formulated as the optimization problem

$$\min_{\overline{x}} \quad \int_0^\infty (S_Z(\omega) - S_X(\omega))^2 d\omega \tag{13}$$

$$s.t. \quad x_j > 0 \quad , j = 1, 2, \cdots, n+m+1 \tag{14}$$

$$\rho^0(0) = 1 \tag{15}$$

where

$$\begin{aligned} \rho^m(\tau) &= \int_{-\infty}^{\infty} (i\omega)^m S_X(\omega) e^{i\omega\tau} d\omega \\ &= 2\pi i \sum_{j=1}^{n} \frac{(i\omega_j)^m e^{i\omega_j\tau} \sum_{k=0}^{m} x_{n+1-k} (i\omega_j)^k \sum_{k=0}^{m} x_{n+1-k} (-i\omega_j)^k}{\prod_{\substack{k=1 \\ k \neq j}}^{2n} (\omega_j - \omega_k)} \end{aligned} \tag{16}$$

is the mth derivative of the correlation coefficient function of $X(t)$. (15) ensures that the standard deviation of $X(t)$ is 1. In the examples in section 5 the optimization problem (13)-(15) is solved using the NLPQL algorithm developed by Schittkowski[12].

In practice the procedure to generate a realization consists of the following steps

a) choose n and m.

b) solve the optimization problem (13)-(15) to determine $\overline{p}$ and $\overline{q}$.

c) compare $S_X(\omega)$ and $S_Z(\omega)$. If the approximation S_X is too good or too bad try new values of n and m and repeat step b, else go to step d.

d) the matrices $\overline{\overline{U}}(\Delta t)$ and $\overline{\overline{T}}$ are determined, see Franklin[9,10].

e) initial values $\overline{\Gamma}(0)$ are determined, see Franklin[9,10].

f) given $\overline{\Gamma}(t)$ and a realization of $\overline{W}$ a new realization of $\overline{\Gamma}(t+\Delta t)$ is determined from (9).

g) a realization of $X(t+\Delta t)$ is determined using (4) and (6) :

$$X(t+\Delta t) = p_0\Gamma^m(t+\Delta t) + p_1\Gamma^{m-1}(t+\Delta t) + \cdots + p_m$$

step f and g are repeated until the realization has the required length.

4 DISTRIBUTION FUNCTIONS OF RANGES

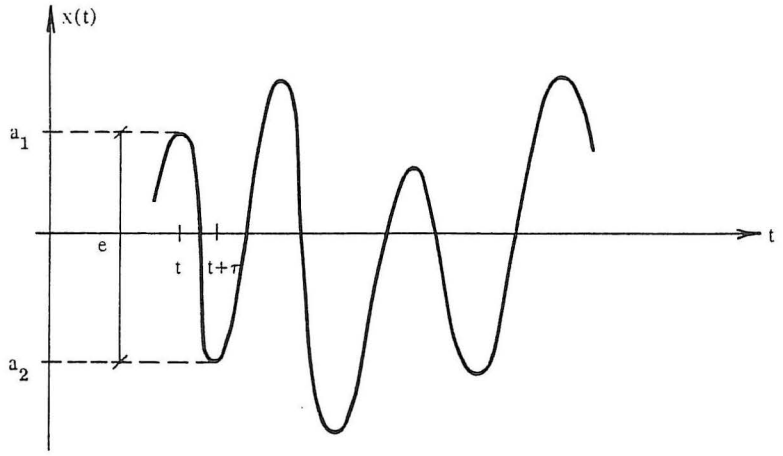

Figure 2. Realization of $X(t)$.

In this section it is described how analytical estimates of the density function of ranges $f_E(e)$ and of the conditional distribution function of ranges given the previous extreme $F_E(e|a_1)$ can be obtained, see fig. 2. The joint distribution function of a peak and a valley with time difference τ is defined by, see Madsen et al.[13]

$$f_{P,V}(a_1,a_2,\tau) = \frac{\int_{-\infty}^{0}\int_{0}^{\infty} -\ddot{x}_1\ddot{x}_2 f_{X_1X_2\dot{X}_1\dot{X}_2\ddot{X}_1\ddot{X}_2}(a_1,a_2,0,0,\ddot{x}_1,\ddot{x}_2)d\ddot{x}_1 d\ddot{x}_2}{\int_{-\infty}^{0}\int_{0}^{\infty} -\ddot{x}_1\ddot{x}_2 f_{\dot{X}_1\dot{X}_2\ddot{X}_1\ddot{X}_2}(0,0,\ddot{x}_1,\ddot{x}_2)d\ddot{x}_1 d\ddot{x}_2} \qquad (17)$$

where $f_{X_1X_2\dot{X}_1\dot{X}_2\ddot{X}_1\ddot{X}_2}$ is the joint density function of $X_1, X_2, \dot{X}_1, \dot{X}_2, \ddot{X}_1$ and $\ddot{X}_2$. Further $X_1 = X(t)$ and $X_2 = X(t+\tau)$. The derivatives $\dot{X}$ and $\ddot{X}$ are assumed to exist. In the appendix it is shown how (17) can be calculated.

In order to estimate the density function of the range between two successive extremes it is also necessary to estimate the density function of times T between successive extremes, $f_T(\tau)$. This is a first passage problem which cannot generally be solved analytically. A

simple estimate of $f_T(\tau)$ can be obtained by using the upper bound

$$f_T(\tau) \leq \int_{-\infty}^{0} \int_{0}^{\infty} -\ddot{x}_1 \ddot{x}_2 f_{\dot{X}_1 \dot{X}_2 \ddot{X}_1 \ddot{X}_2}(0,0,\ddot{x}_1,\ddot{x}_2) d\ddot{x}_1 \; d\ddot{x}_2 \tag{18}$$

(18) is used in the interval $0 \leq \tau \leq T_0$ where T_0 is determined from the normalization condition

$$\int_0^{T_0} f_T(\tau) d\tau = 1 \tag{19}$$

When $\tau > T_0$ we use $f_T(\tau) = 0$.

From (17) and (18) the density function f_E of the range between two successive extremes can be estimated by

$$f_E(e) = \int_0^{\infty} f_T(\tau) \int_{-\infty}^{\infty} f_{P,V}(a, a-e, \tau) da \; d\tau \tag{20}$$

(20) can be calculated by numerical integration. The distribution function $F_E(e|a_1)$ of the range E given the peak a_1 is estimated from

$$F_E(e|a_1) = \frac{\int_{-\infty}^{e} \int_0^{\infty} f_{P,V}(a_1, a_1 - x, \tau) f_T(\tau) d\tau dx}{f_P(a_1)} \tag{21}$$

In (21) the density function $f_P(a)$ of a single peak is given by

$$\begin{aligned} f_P(a) &= \frac{\int_{-\infty}^{0} -\ddot{x} f_{X\dot{X}\ddot{X}}(a, o, \ddot{x}) d\ddot{x}}{\int_{-\infty}^{0} -\ddot{x} f_{\dot{X}\ddot{X}}(o, \ddot{x}) d\ddot{x}} \\ &= -\frac{\sqrt{R}}{\sqrt{\rho^4(0)}} exp(-\frac{1}{2}a^2) \int_{-\infty}^{-\frac{a\rho^2(0)}{\sqrt{R}}} (y + \frac{a\rho^2(0)}{\sqrt{R}}) \varphi(y) dy \end{aligned} \tag{22}$$

where

$$R = \rho^4(0) - (\rho^2(0))^2 \tag{23}$$

and $\varphi(\cdot)$ is the normalized normal density function.

As described in section 2 (21) can be used as the basis of simulation of successive extremes of a fatigue load process. If the influence of the latest estreme on the range is neglected (20) can be used as the basis of the simulation.

5 EXAMPLE

In this example we consider two tubular joints in a 3-dimensional model of an offshore steel-jacket platform analysed in Sigurdsson[14]. The structure is loaded mainly by waves with frequencies about $\omega = 0.6$ $[rad/sec]$ and has the lowest eigenfrequency $\omega_1 = 3.0$ $[rad/sec]$. In figures 3 and 4 the stress spectra are shown for the two joints for two different load cases. The spectra are normalized to unit standard deviation. Estimates of the spectra are calculated in Sigurdsson[14] at a number of discrete frequencies and are shown in the figures as vertical lines. Also shown are approximations of the spectra by rational spectra, see (3). The rational spectra are shown by continuous lines. In both spectra n=8 and m=3 are used. The spectra are characterized by the parameter ϵ defined by

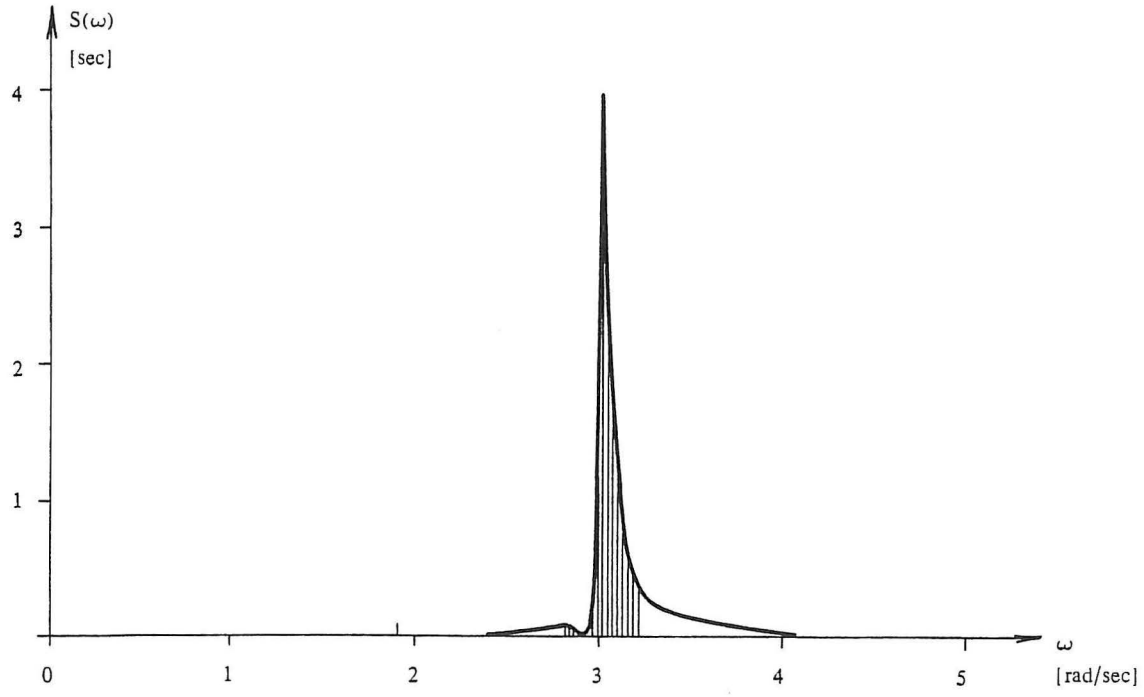

Figure 3. Spectrum "narrow". Vertical lines : estimates from Sigurdsson[14]. Continuous line : approximation by rational spectrum, n = 8 and m = 3. $\epsilon = 0.2$.

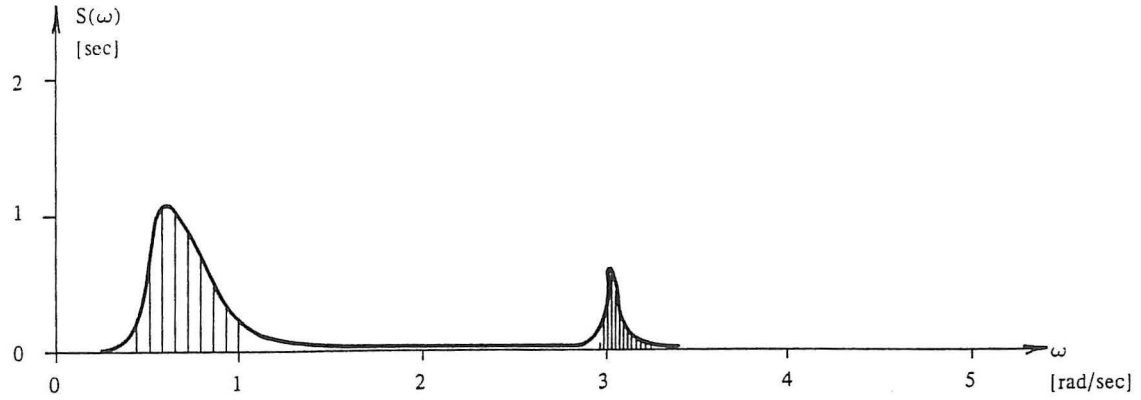

Figure 4. Spectrum "wide". Vertical lines : estimates from Sigurdsson[14]. Continuous line : approximation by rational spectrum, n = 8 and m = 3. $\epsilon = 0.8$.

$$\epsilon = \sqrt{1 - \frac{m_2^2}{m_0 m_4}} \tag{24}$$

where m_j is the j th spectral moment

$$m_j = 2 \int_0^\infty \omega^j S(\omega) d\omega \tag{25}$$

ϵ close to 0 and 1 indicate a narrow-banded and a wide-banded spectrum, respectively. The spectra in figure 3 and 4 have $\epsilon = 0.2$ and $\epsilon = 0.8$. Therefore, they can be characterized as "narrow" and "wide", respectively.

In figure 5 and 6 estimates of the density function f_T of times between successive extremes are shown by continuous lines. The estimates are calculated using the approximation (18) and the approximate rational spectra. Also shown in figure 5 and 6 are simulation estimates. The simulations are performed using the method described in section 3 with Δt=0.1 sec. and a total simulated time length of 60000 sec. It is seen that in both figures the deviations are small between the upper bound (18) with cut-off at T_0 and the simulation results.

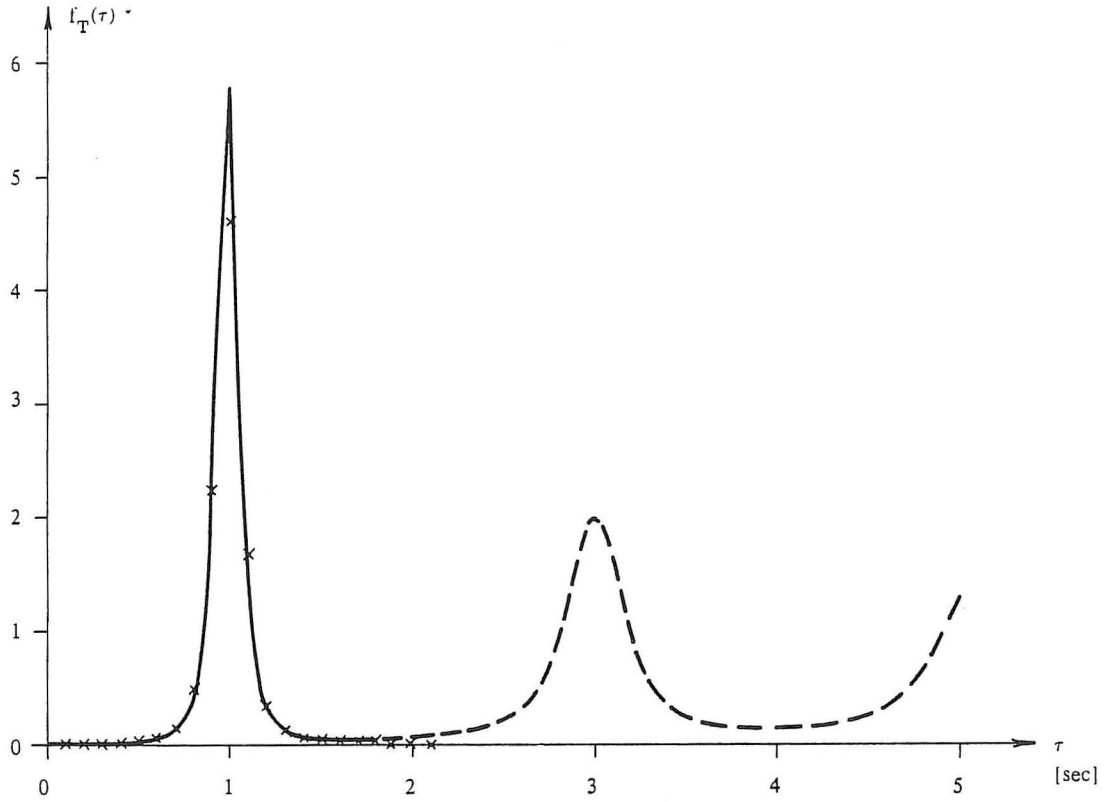

Figure 5. "Narrow" spectrum : estimate of $f_T(\tau)$ by (18). The start of the broken line indicates the time T_0. Simulation results are indicated by $\times$.

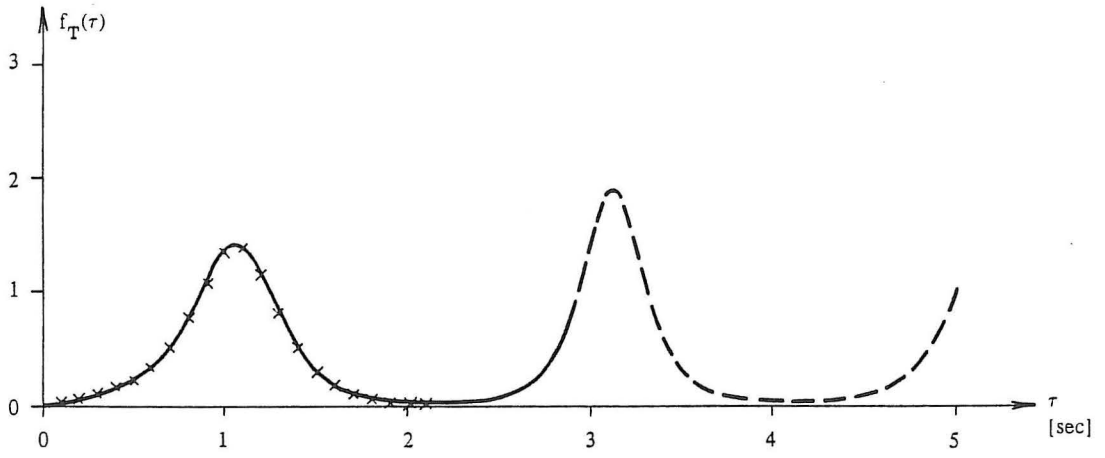

Figure 6. "Wide" spectrum : estimate of $f_T(\tau)$ by (18). The start of the broken line indicates the time T_0. Simulation results are indicated by $\times$.

In figures 7 and 8 analytical estimates of the conditional distribution function $F_E(e|a^l \leq a_1 \leq a^u)$ calculated using (21) are compared with simulation results. Four different intervals of the previous extreme are considered. Figure 7 shows that in the case of a narrow-banded spectrum the analytical estimates correspond very well to the simulation results.

For the wide-banded spectrum figure 8 shows that some deviation occurs for distributions conditioned on high previous extremes.

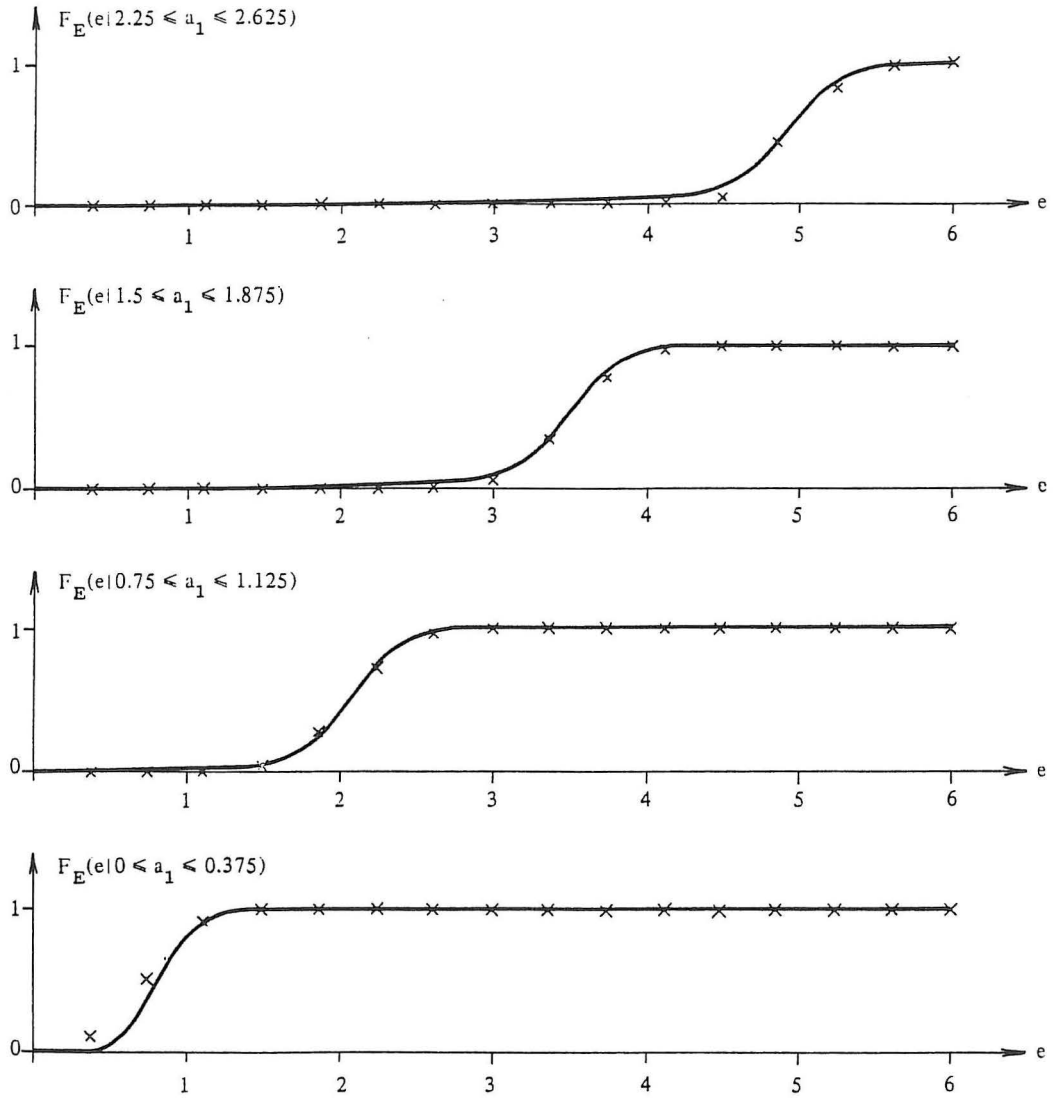

Figure 7. "Narrow" spectrum : conditional distribution functions $F_E(e|a^l \leq a_1 \leq a^u)$ estimated by (21). Simulation results are indicated by $\times$.

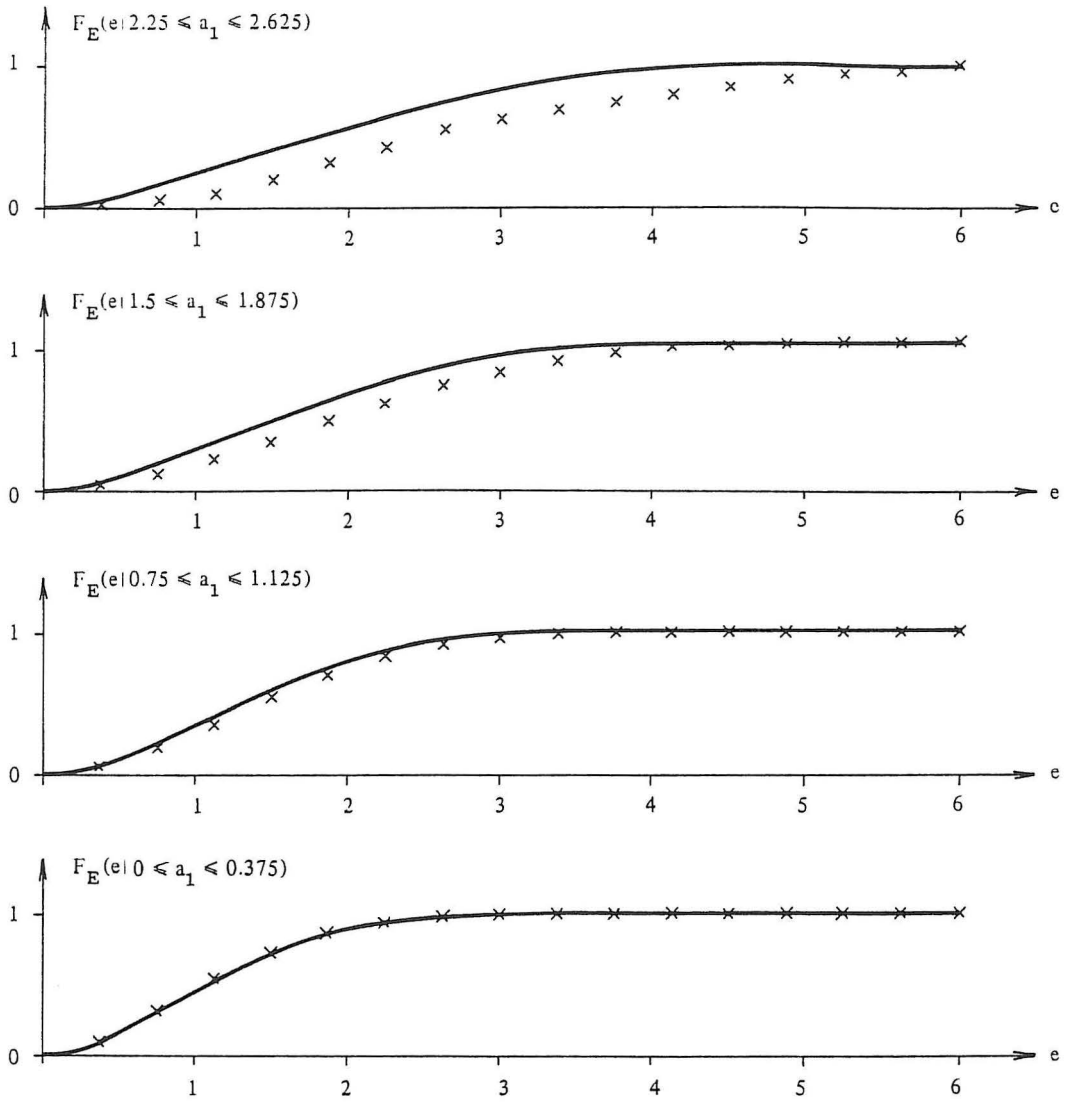

Figure 8. "Wide" spectrum : conditional distribution functions $F_E(e|a^l \leq a_1 \leq a^u)$ estimated by (21). Simulation results are indicated by $\times$.

In figures 9 and 10 estimates of the density function $f_E(e)$ of ranges between successive exrtremes calculated using (20) are compared with simulation results. • indicates simulation estimates of the density function of ranges between successive extremes. Also shown in the figures are simulation results indicated by $\times$. These estimates are based on ranges obtained by performing Rainflow counting, see Madsen et al.[13]. Rainflow counting is generally accepted to give good estimates of the density functions of ranges and expected number of ranges to be used in practical fatigue analyses. In the case of a narrow-banded spectrum there is very close agreement between analytical estimates and simulation results. For the wide-banded spectrum the estimates based on Rainflow counting are significantly different

from the analytical estimates and the simulation estimates based on range counting.

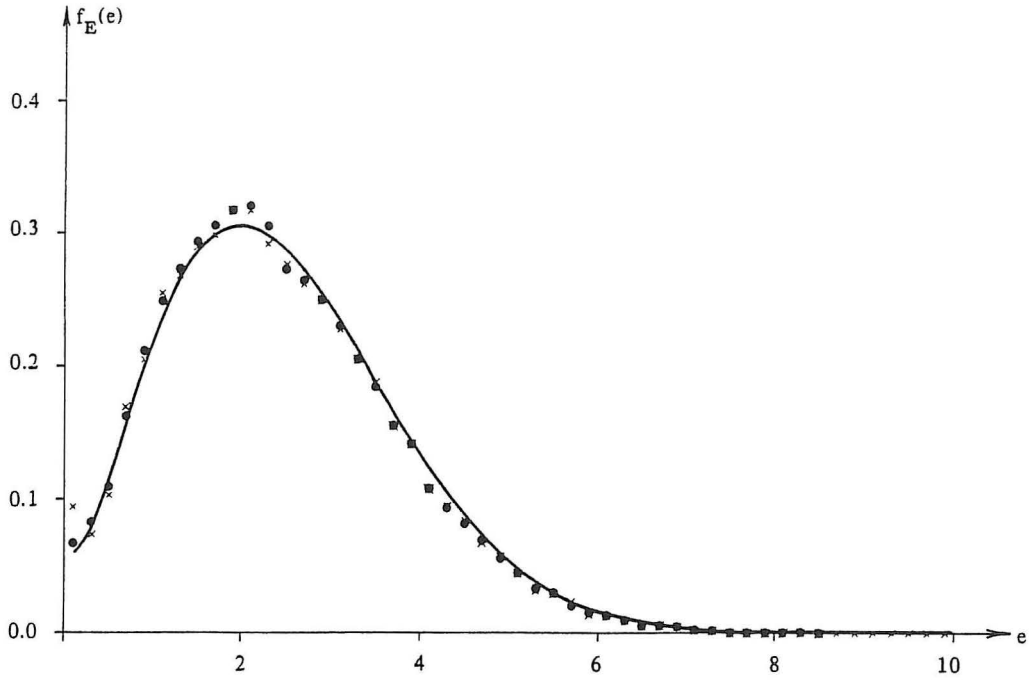

Figure 9. "Narrow" spectrum : density function $f_E(e)$ estimated by (20). Simulation results are indicated by • and ×.

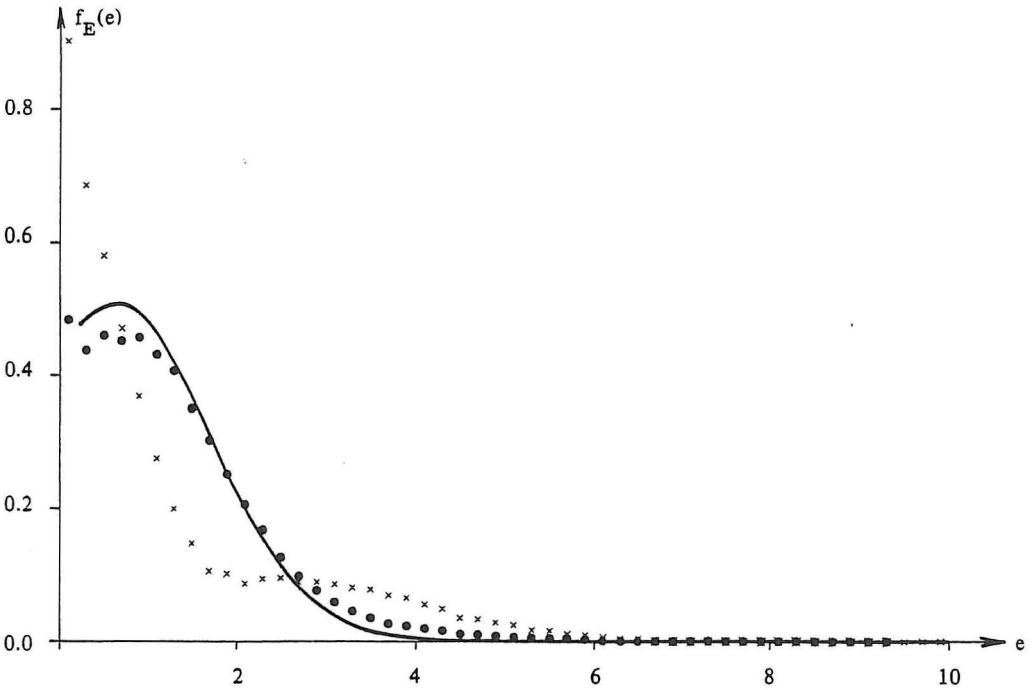

Figure 10. "Wide" spectrum : density function $f_E(e)$ estimated by (20). Simulation results are indicated by • and ×.

In order to investigate the simple direct simulation method for fatigue tests proposed in section 2 some simulations have been performed using this method. Only extremes within the interval $[-3, 3]$ have been considered. The interval has been discretized into 16 uniformly distributed points. It is then possible to estimate a jump matrix (see section 2) with 16×16 elements. Each of the elements gives the range to the next extreme given an extreme (peak or valley). Each of the elements are estimated by simulation.

In figures 11 and 12 simulation results are shown obtained by the simple direct simulation method. o and + indicate estimates of the density of ranges between successive extremes and estimates based on Rainflow counting. For the narrow-banded spectrum there are only small differences between the estimates obtained by the two methods. The results for the wide-banded spectrum show greater differences between the estimates of the two simulation methods. But still the differences are not significant (see also figures 13-20). The differences are most obvious for the Rainflow counting estimates and are most probably due to the fact that the simple simulation method is not able to reproduce realizations where the next extreme is dependent of more than the latest extreme.

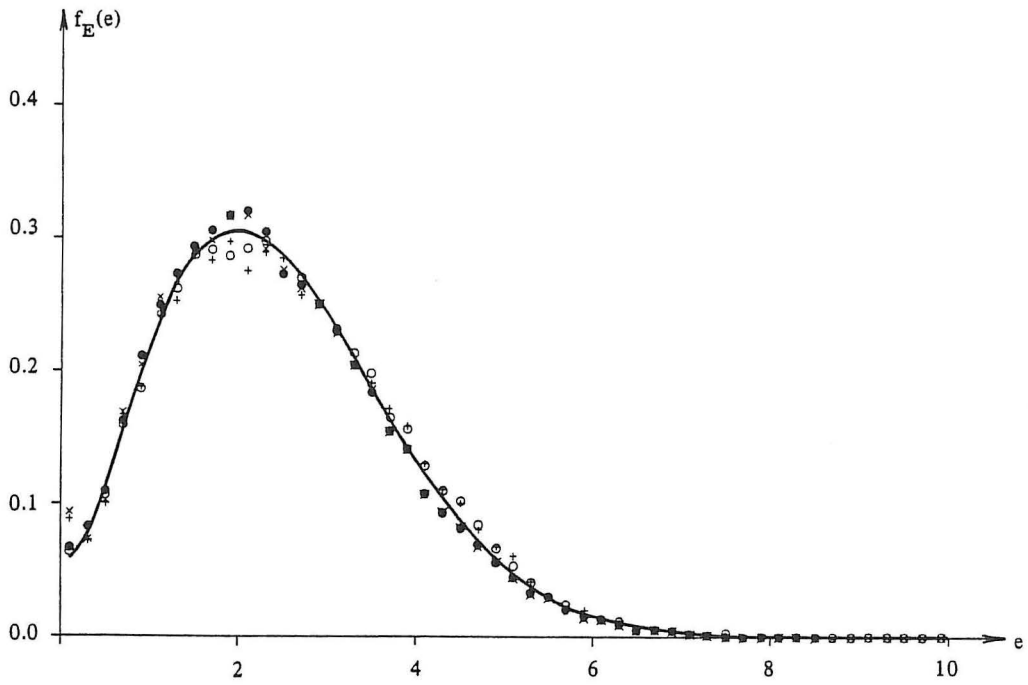

Figure 11. "Narrow" spectrum : density function $f_E(e)$ estimated by (20). Simulation results are indicated by $\bullet, \times, o$ and $+$.

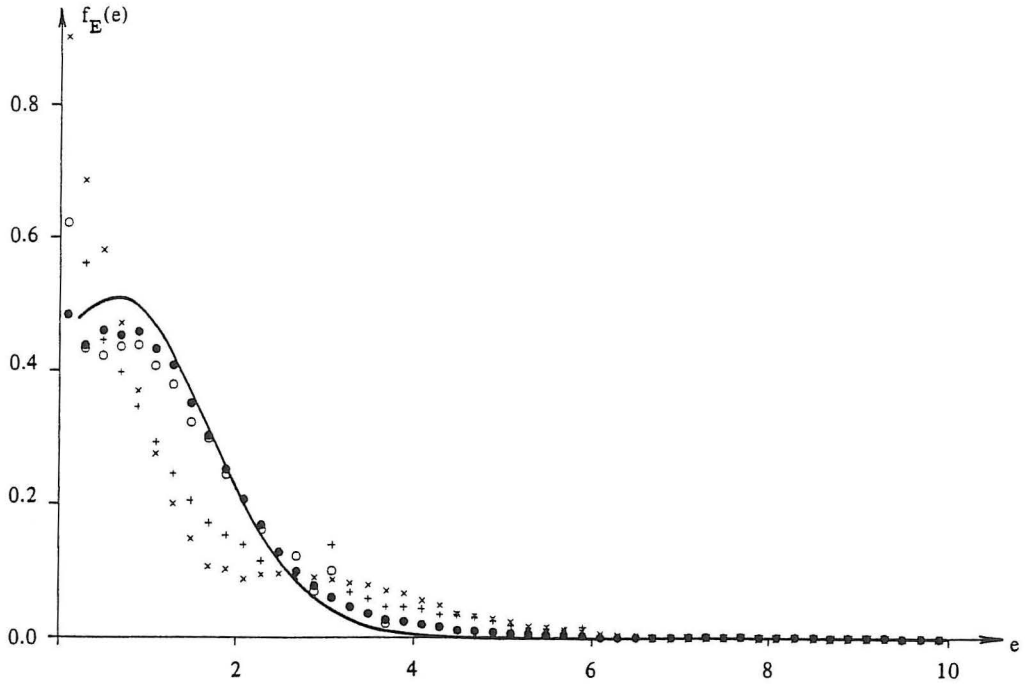

Figure 12. "Wide" spectrum : density function $f_E(e)$ estimated by (20). Simulation results are indicated by •,×,○ and +.

Finally the simple direct simulation method to be used to generate load realizations in fatigue experiments is tested by comparing the fatigue lives of a simple model. Let a and N model the crack length and the number of stress ranges. Then in linear elastic fracture mechanics the increase in crack length Δa for each load cycle can in some simple cases be determined by, see Madsen et al.[13]

$$\Delta a = c(b\Delta\sigma\sqrt{\pi a})^{m_1} \tag{26}$$

where c and m_1 are material parameters. b is a constant and $\Delta\sigma$ is the range between successive extremes of the load process. c,m_1 and b are assumed to be deterministic. The initial length and the critical crack length are modelled by a_0 and a_{cr}. In the following example we use $c = 1.92\ 10^{-13}, m_1 = 3, b = 100, a_0 = 2$ and $a_{cr} = 50$ (dimensions omitted)

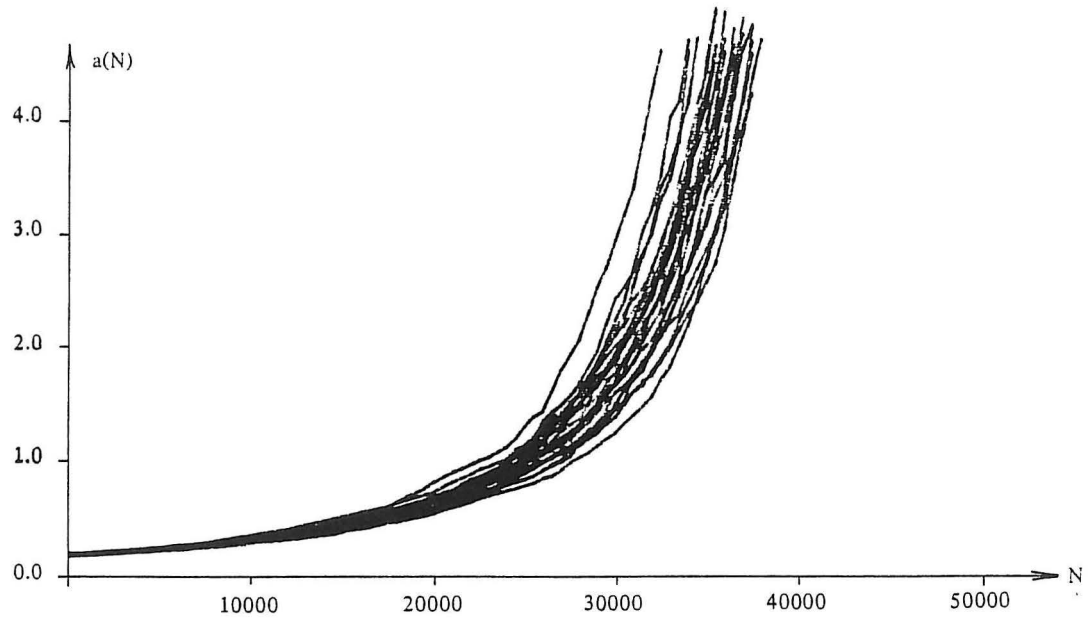

Figure 13. "Narrow" spectrum : crack length as a function of the number of load cycles N. "Exact simulation" and range counting. $E[N_{cr}] = 36300, \sigma[N_{cr}] = 1300$.

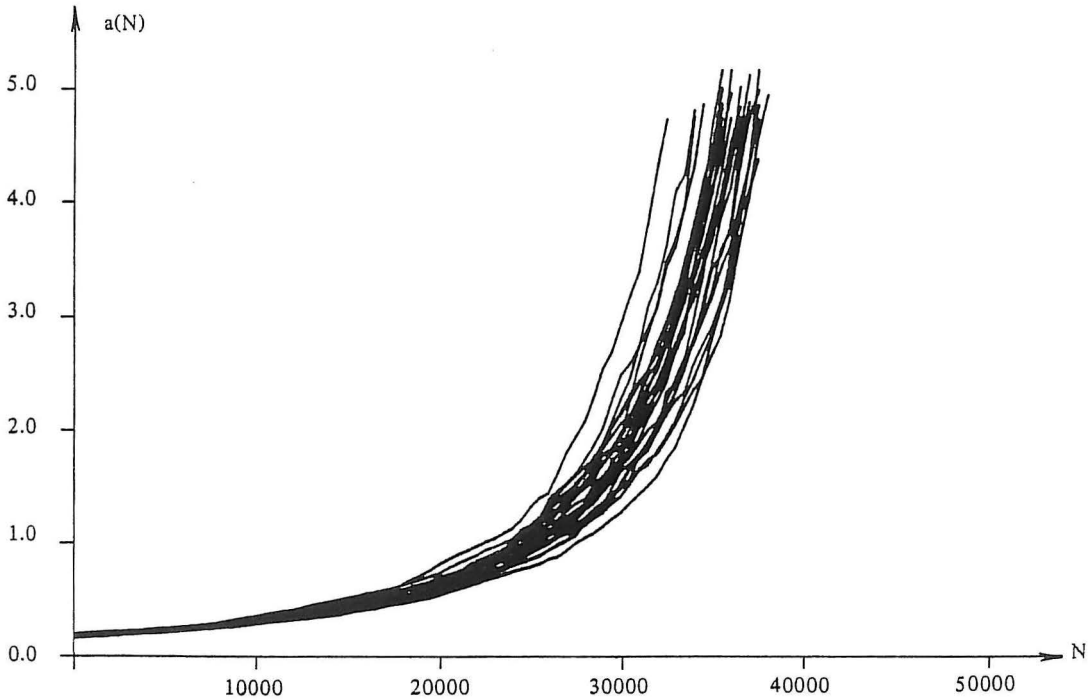

Figure 14. "Narrow" spectrum : crack length as a function of the number of load cycles N. "Exact simulation" and Rainflow counting. $E[N_{cr}] = 36200, \sigma[N_{cr}] = 1300$.

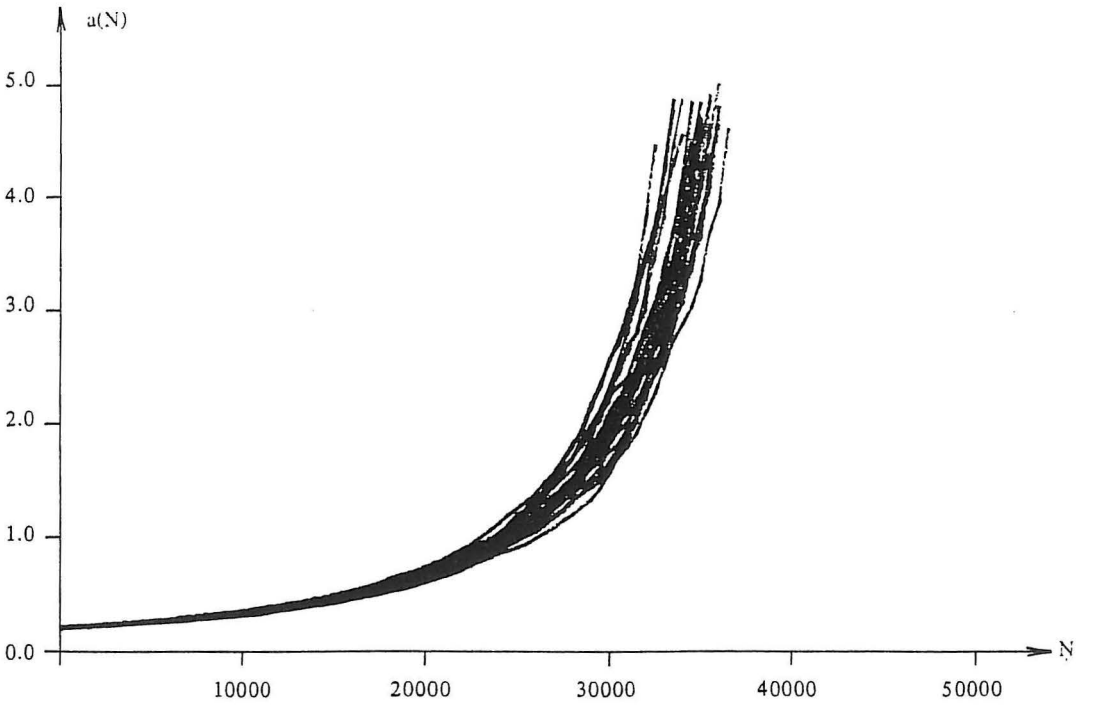

Figure 15. "Narrow" spectrum : crack length as a function of the number of load cycles N. "Simple simulation" and range counting. $E[N_{cr}] = 35200, \sigma[N_{cr}] = 900$.

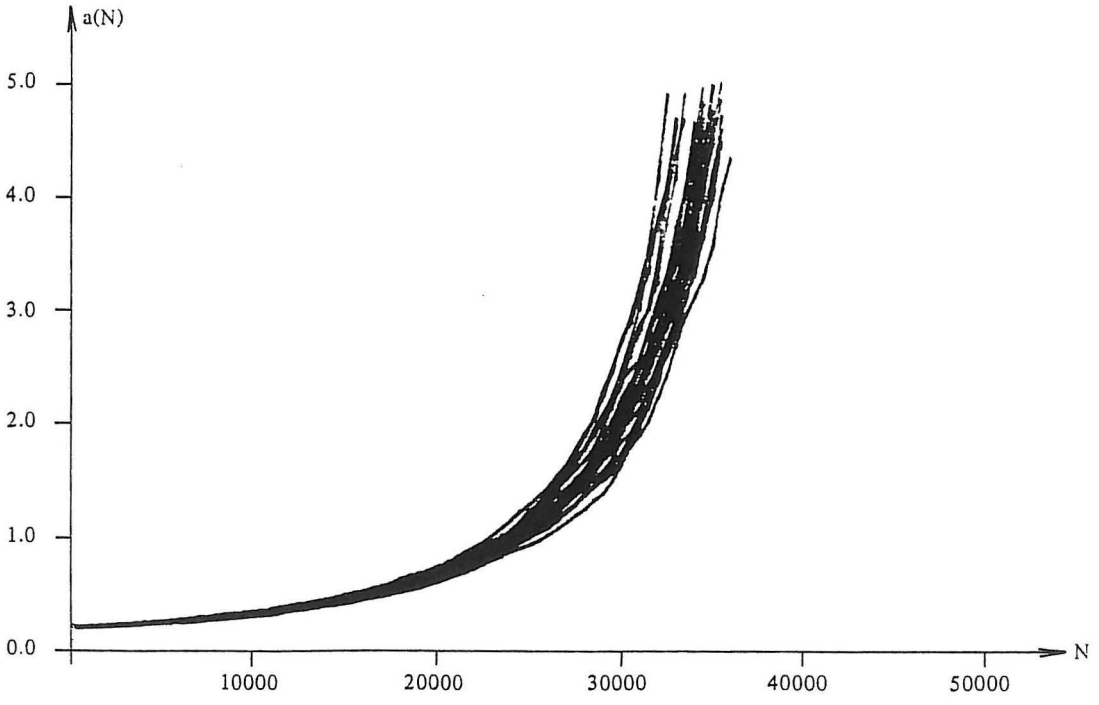

Figure 16. "Narrow" spectrum : crack length as a function of the number of load cycles N. "Simple simulation" and Rainflow counting. $E[N_{cr}] = 34800, \sigma[N_{cr}] = 900$.

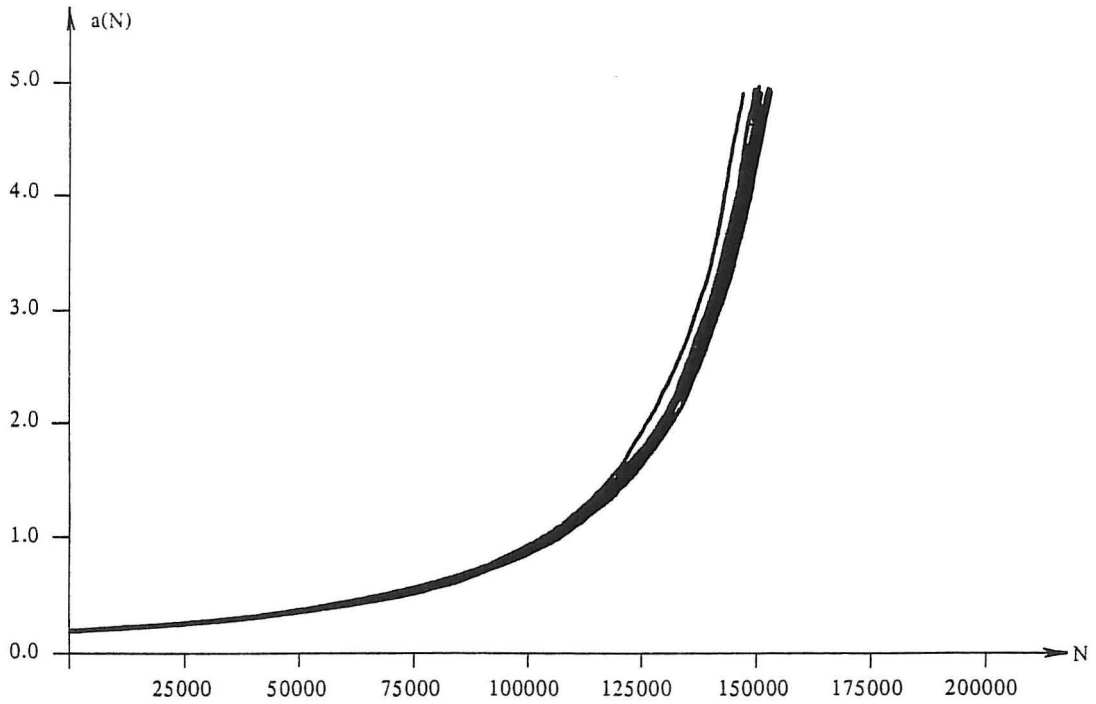

Figure 17. "Wide" spectrum : crack length as a function of the number of load cycles N. "Exact simulation" and range counting. $E[N_{cr}] = 152000, \sigma[N_{cr}] = 1830$.

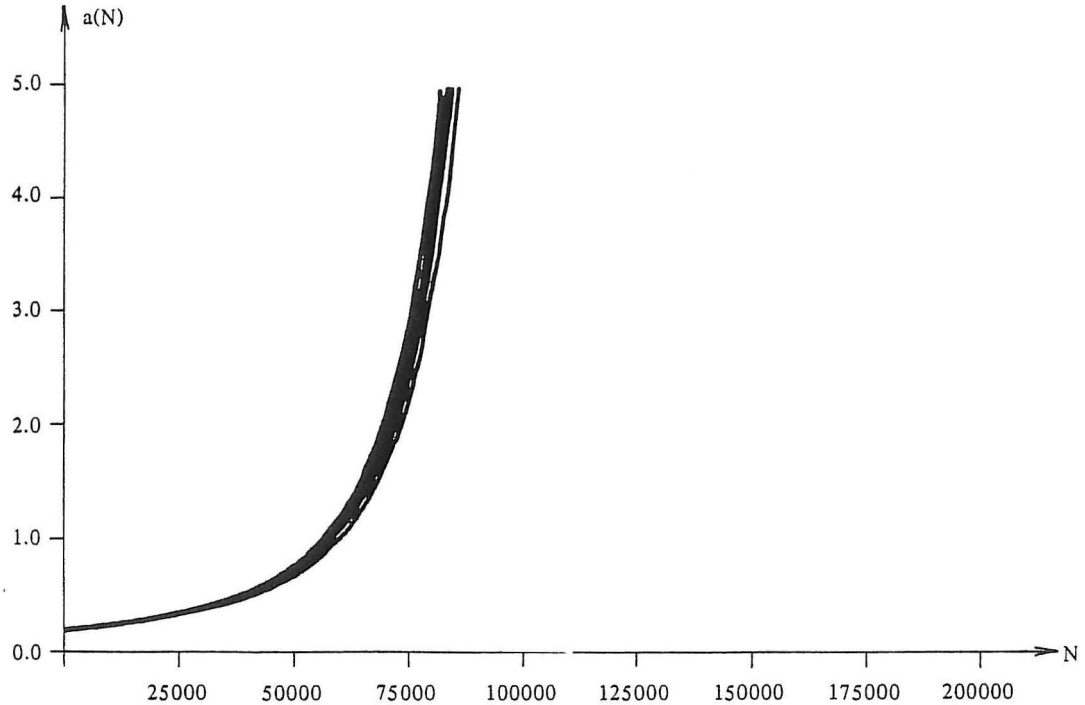

Figure 18. "Wide" spectrum : crack length as a function of the number of load cycles N. "Exact simulation" and Rainflow counting. $E[N_{cr}] = 83100, \sigma[N_{cr}] = 1250$.

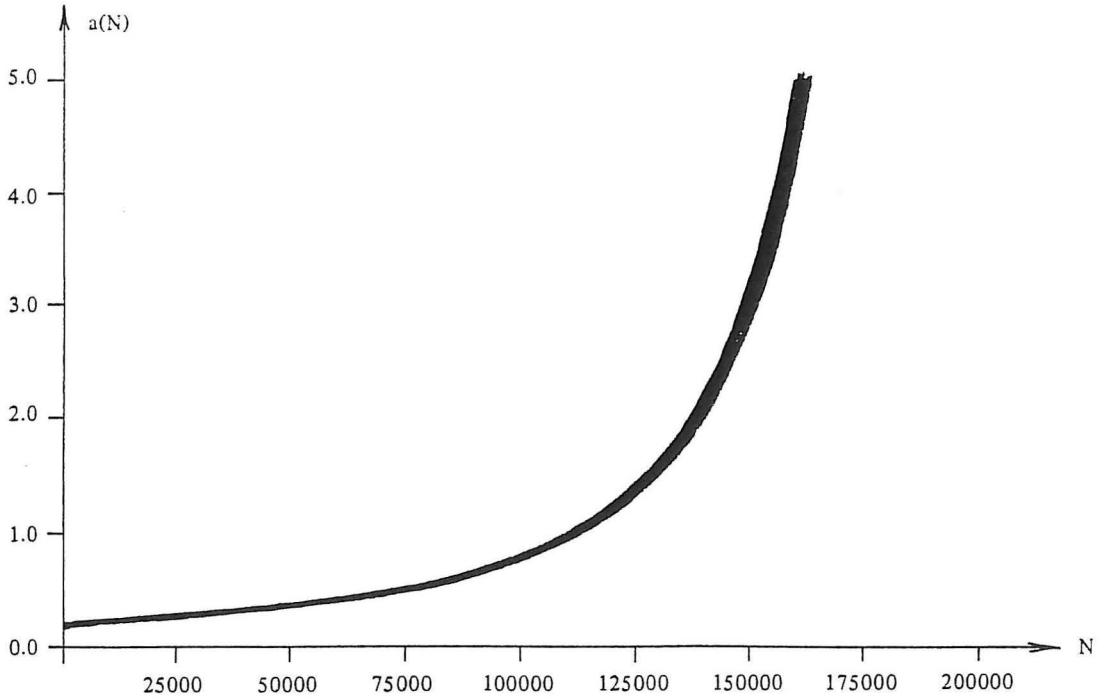

Figure 19. "Wide" spectrum : crack length as a function of the number of load cycles N. "Simple simulation" and range counting. $E[N_{cr}] = 161000, \sigma[N_{cr}] = 830$.

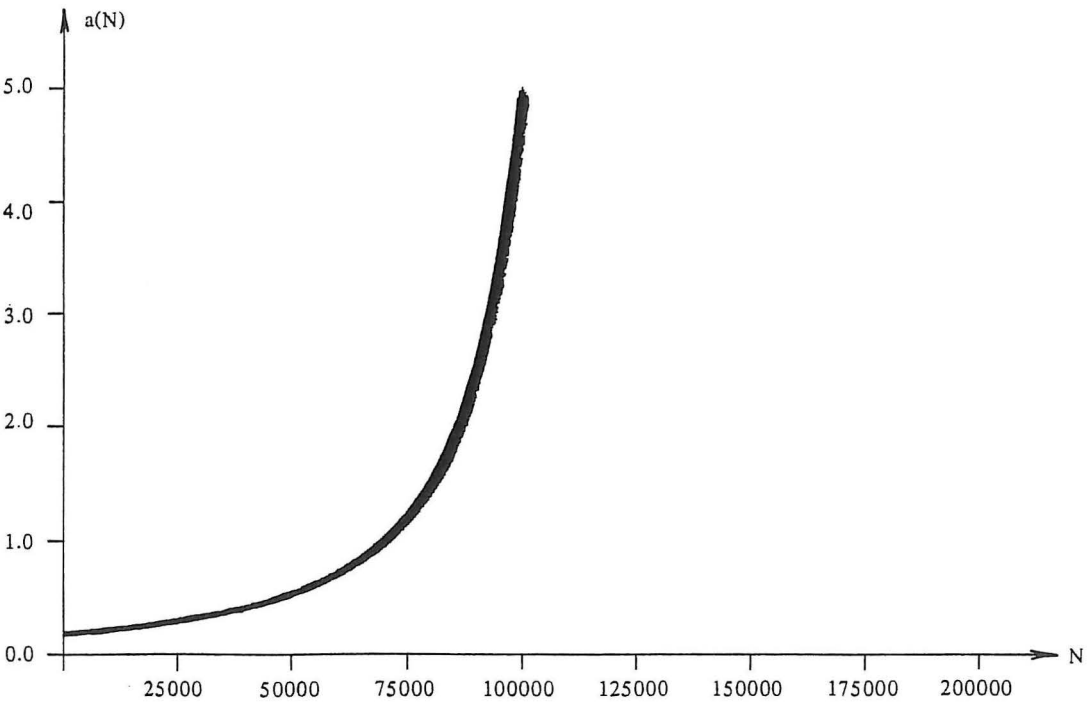

Figure 20. "Wide" spectrum : crack length as a function of the number of load cycles N. "Simple simulation" and Rainflow counting. $E[N_{cr}] = 100300, \sigma[N_{cr}] = 680$.

In figures 13-20 simulation results show the crack length as a function of the number of load cycles. For the narrow-banded spectrum it is seen that the same critical number of load cycles N_{cr} is obtained for the "exact" simulation method described in section 3 and the simple direct simulation method proposed in section 2 both for range and Rainflow counting based methods. Each figure is based on 25 simulations. Figures 17-20 show the results for the wide-banded spectrum based on 10 simulations. The results show that significant differences for N_{cr} are obtained for the range and Rainflow counting method but the two simulation methods give nearly the same estimates. From these crack length simulations it can be concluded that the simple direct fatigue load simulation method is able to produce realizations which result in nearly the same fatigue life as realizations simulated using the much more advanced simulation method described in section 3. If the single crack length realizations are compared the same conclusion can be drawn.

In addition it appears from the realizations that the narrow-banded spectrum results in much more fluctuating realizations than the wide-banded spectrum.

	Rainflow counting		Range counting	
	μ	σ	μ	σ
"Narrow" spectrum				
"exact" simulation	36200	1300	36300	1300
"simple" simulation N=8	40000	600	41300	650
"simple" simulation N=16	34800	900	35200	900
"simple" simulation N=32	36000	570	37100	600
"Wide" spectrum				
"exact" simulation	83100	1250	152000	1830
"simple" simulation N=8	124200	770	194600	1130
"simple" simulation N=16	100300	680	161000	830
"simple" simulation N=32	94700	600	152700	750

Table 1. Number of load cycles N_{cr} corresponding to failure. μ : expected value, σ : standard deviation.

In table 1 the critical numbers of load cycles N_{cr} are shown for "exact" simulation and "simple" simulation for different discretizations N=8,16 and 32. All estimates are based on 25 realizations. From the table it appears that increasing the discretization degree in the simple direct simulation method generally implies that the estimates of N_{cr} approach the estimates obtained by "exact" simulation. A discretization with N=32 is seen to give satisfactory results in most cases.

7 CONCLUSION

In this paper an efficient and simple method to simulate realizations of stochastic loads for fatigue experiments is presented. The method is based on the assumption that for most fatigue experiments it is sufficient to describe the realizations by the extreme values of the load. A simple method is proposed where the range between two successive extremes is assumed only to depend on the value of the latest extreme. Realizations can thus be generated if the conditional distribution function of the range given the latest extreme is known.

Two methods to estimate the conditional distribution function are described. The first method is based on an analytical approximation to the first-passage problem which it is necessary to solve to estimate the conditional distribution function. Numerical examples indicate that for two stochatic processes described by quite different spectra the approximation gives results which agree well with simulation results. The second method is based on estimates determined from a more accurate simulation method which is based on a Markov approximation of the spectrum of the stochastic process describing the fatigue load.

The simple fatigue load simulation method is compared with the more accurate simulation method in an example where the fatigue crack length growth is described by a simple model. The example shows that the simple simulation method for the two spectra considered is able to describe the fatigue crack growth with sufficient accuracy.

8 REFERENCES

[1] Madsen, H.O. : Deterministic and Probabilistic Models for Damage Accumulation Due to Time Varying Loading. DIALOG 5-82, Danish Engineering Academy, Lyngby, Denmark, 1982.

[2] Sobczyk, K. : Modelling of Random Fatigue Crack Growth. Engineering Fracture Mechanics, Vol. 24, No. 4, 1986, pp. 609-623.

[3] Brincker, R. & J.D. Sørensen : High Speed Fatigue Stochastic Testing. Submitted to Experimental Mechanics, 1987.

[4] Borgman, L.E. : Ocean Wave Simulation for Engineering Design. Journal of the Waterways and Harbours Division, ASCE, Vol. 95, No. WW4, 1969,pp. 557-583.

[5] Yang, J.-N. : On the Normality and Accuracy of Simulated Random Processes. Journal of Sound and Vibration, Vol. 26, No. 3, 1973, pp. 417-428.

[6] Box, G.E.P. & G.M. Jenkins : Time Series Analysis : Forecasting and Control. Holden-Day, San Francisco, 1976.

[7] Clang, M.K., J.W. Kwiatkowski & R.F. Nau : ARMA Models for Earthquake Ground

Motions. Earthquake Engineering and Structural Dynamics, Vol. 10, 1982, pp. 651-662.

[8] Krenk, S. & J. Clausen : On the Calibration of ARMA Processes for Simulation. Proc. IFIP WG 7.5, Springer Verlag, 1987, pp. 243-257.

[9] Franklin, J.N. : Numerical Simulation of Stationary and Nonstationary Gaussian Random Processes. SIAM Review, Vol. 7, No. 1, 1965, pp. 68-80.

[10] Franklin, J.N. : The Covariance Matrix of a Continuous Autoregressive Vector Time-Series. Ann. Math. Stat., Vol. 34, 1963, pp. 1259-1264.

[11] Hammersley, J.M. & D.C. Handscomb : Monte Carlo Methods, Methuen, London, 1964.

[12] Schittkowski, K. : NLPQL : A FORTRAN Subroutine Solving Constrained Non-Linear Programming Problems. Annals of Operations Research, 1986.

[13] Madsen, H.O., S. Krenk & N.C. Lind : Methods of Structural Safety. Prentice-Hall, 1986.

[14] Sigurdsson, G. : Development of Applicable Methods for Evaluating the Safety of Offshore Structures, Part 4. Structural Reliability Theory, Paper No. 24, The University of Aalborg, Denmark,1987.

APPENDIX : Calculation of $f_{P,V}(a_1, a_2, \tau)$

The joint density function in (17) can be written

$$f_{P,V}(a_1, a_2, \tau) = \frac{\int_{-\infty}^{0}\int_{0}^{\infty} -\ddot{x}_1\ddot{x}_2\varphi_6(a_1, a_2, 0, 0, \ddot{x}_1, \ddot{x}_2; \bar{\bar{\rho}}_1)d\ddot{x}_1 d\ddot{x}_2}{\int_{-\infty}^{0}\int_{0}^{\infty} -\ddot{x}_1\ddot{x}_2\varphi_4(0, 0, \ddot{x}_1, \ddot{x}_2; \bar{\bar{\rho}}_2)d\ddot{x}_1 d\ddot{x}_2} = \frac{A}{B} \qquad (A1)$$

where $\varphi_n(\cdot, \bar{\bar{\rho}})$ is the n-dimensional normalized normal density function of n variables having the correlation coefficient matrix $\bar{\bar{\rho}}$. $\bar{\bar{\rho}}_1$ is written

$$\bar{\bar{\rho}}_1 = \left(\begin{array}{cccc|cc} 1 & \rho(\tau) & 0 & \rho^1(\tau) & \rho^2(0) & \rho^2(\tau) \\ \rho(\tau) & 1 & -\rho^1(\tau) & 0 & \rho^2(\tau) & \rho^2(0) \\ 0 & -\rho^1(\tau) & -\rho^2(0) & -\rho^2(\tau) & 0 & -\rho^3(\tau) \\ \rho^1(\tau) & 0 & -\rho^2(\tau) & -\rho^2(0) & \rho^3(\tau) & 0 \\ - & - & - & - & - & - \\ \rho^2(0) & \rho^2(\tau) & 0 & \rho^3(\tau) & \rho^4(0) & \rho^4(\tau) \\ \rho^2(\tau) & \rho^2(0) & -\rho^3(\tau) & 0 & \rho^4(\tau) & \rho^4(0) \end{array}\right) = \left(\begin{array}{cc} \bar{\bar{\rho}}_{11} & \bar{\bar{\rho}}_{12} \\ \bar{\bar{\rho}}_{12}^T & \bar{\bar{\rho}}_{22} \end{array}\right) \qquad (A2)$$

A can be written

$$A = -\varphi_4(a_1, a_2, 0, 0; \bar{\bar{\rho}}_{11}) \int_{-\infty}^{0} \int_{0}^{\infty} \ddot{x}_1 \ddot{x}_2 \varphi_2(\ddot{x}_1 - \mu_1, \ddot{x}_2 - \mu_2; \bar{\bar{R}}) d\ddot{x}_1 d\ddot{x}_2$$
$$= -\varphi_4(a_1, a_2, 0, 0; \bar{\bar{\rho}}_{11}) \lambda_1 \lambda_2 \Big[-\Psi_2(-\frac{\mu_1}{\lambda_1}) \Psi_1(-\frac{\mu_2}{\lambda_2}) - \kappa \Phi(-\frac{\mu_1}{\lambda_1}) \Phi(\frac{\mu_2}{\lambda_2})$$
$$+ \lambda_1 \lambda_2 \int_0^{\kappa} (\kappa - k) \varphi_2(0, 0; \bar{\bar{R}}(k)) dk \Big] \qquad (A3)$$

where

$$\bar{\mu} = \begin{pmatrix} \mu_1 \\ \mu_2 \end{pmatrix} = \bar{\bar{\rho}}_{12}^T \bar{\bar{\rho}}_{11}^{-1} \begin{pmatrix} a_1 \\ a_2 \\ 0 \\ 0 \end{pmatrix} \qquad (A4)$$

$$\bar{\bar{R}}(\kappa) = \bar{\bar{\rho}}_{22} - \bar{\bar{\rho}}_{12}^T \bar{\bar{\rho}}_{11}^{-1} \bar{\bar{\rho}}_{12} = \begin{pmatrix} \lambda_1^2 & \kappa \lambda_1 \lambda_2 \\ \kappa \lambda_1 \lambda_2 & \lambda_2^2 \end{pmatrix} \qquad (A5)$$

$$\Psi_1(x) = \varphi(x) - x\Phi(-x) \qquad (A6)$$

$$\Psi_2(x) = -\varphi(x) - x\Phi(x) \qquad (A7)$$

$\Phi(\cdot)$ is the standard normal distribution function. λ_1, λ_2 and κ are defined by (A5).

ρ_2 is written

$$\bar{\bar{\rho}}_2 = \left(\begin{array}{cccc} -\rho^2(0) & -\rho^2(\tau) & 0 & -\rho^3(\tau) \\ -\rho^2(\tau) & -\rho^2(0) & \rho^3(\tau) & 0 \\ - & - & - & - \\ 0 & \rho^3(\tau) & \rho^4(0) & \rho^4(\tau) \\ -\rho^3(\tau) & 0 & \rho^4(\tau) & \rho^4(0) \end{array} \right) = \begin{pmatrix} \bar{\bar{r}}_{11} & \bar{\bar{r}}_{12} \\ \bar{\bar{r}}_{12}^T & \bar{\bar{r}}_{22} \end{pmatrix} \qquad (A8)$$

B in (A1) can then be written

$$B = -\varphi_2(0, 0; \bar{\bar{r}}_{11}) \int_{-\infty}^{0} \int_{0}^{\infty} \ddot{x}_1 \ddot{x}_2 \varphi_2(\ddot{x}_1, \ddot{x}_2; \bar{\bar{r}}) d\ddot{x}_1 d\ddot{x}_2$$
$$= -\varphi_2(0, 0; \bar{\bar{r}}_{11}) \lambda_1 \lambda_2 \Big[-\Psi_2(0) \Psi_1(0) - \frac{\kappa}{4} + \lambda_1 \lambda_2 \int_0^{\kappa} (\kappa - k) \varphi_2(0, 0; \bar{\bar{r}}(k)) dk \Big] \qquad (A9)$$

where

$$\bar{\bar{r}}(\kappa) = \bar{\bar{r}}_{22} - \bar{\bar{r}}_{12}^T \bar{\bar{r}}_{11}^{-1} \bar{\bar{r}}_{12} = \begin{pmatrix} \lambda_1^2 & \kappa \lambda_1 \lambda_2 \\ \kappa \lambda_1 \lambda_2 & \lambda_2^2 \end{pmatrix} \qquad (A10)$$

STRUCTURAL RELIABILITY THEORY SERIES

PAPER NO. 1: J. D. Sørensen & P. Thoft-Christensen: *Model Uncertainty for Bilinear Hysteretic Systems*, IFB/A 8302.

PAPER NO. 2: P. Thoft-Christensen & J. D. Sørensen: *Reliability Analysis of Elasto-Plastic Structures*, IFB/A 8303.

PAPER NO. 3: P. Thoft-Christensen: *Reliability Analysis of Structural Systems by the β-Unzipping Method.* (Preprint of a chapter of the new textbook: »Reliability of Structural Systems») ISSN 0105-7421 R8401.

PAPER NO. 4: J. D. Sørensen: *Pålidelighedsanalyse af statisk og dynamisk belastede elasto-plastiske ramme- og gitterkonstruktioner.* ISSN 0105-7421 R8402. (Ph.D. Thesis - in Danish).

PAPER NO. 5: P. Thoft-Christensen: *Reliability of Structural Systems.* ISSN 0105-7421 R8403.

PAPER NO. 6: P. Thoft-Christensen & J. D. Sørensen: *Optimization and Reliability of Structural Systems.* ISSN 0105-7421 R8404.

PAPER NO. 7: P. Thoft-Christensen & J. D. Sørensen: *A Bibliographical Survey of Structural Reliability.* 1st edition. ISSN 0105-7421 R8408.

PAPER NO. 8: P. Thoft-Christensen: *Structural Reliability Theory.* ISSN 0105-7421 R8409.

PAPER NO. 9: G. Sigurdsson, J. D. Sørensen & P. Thoft-Christensen: *Development of Methods for Evaluating the Safety of Offshore Structures, Part 1.* ISSN 0105-7421 R8501.

PAPER NO. 10: J. D. Sørensen & P. Thoft-Christensen: *Modelling and Simulation of Wave Loads.* ISSN 0105-7421 R8503.

PAPER NO. 11: J. D. Sørensen, P. Thoft-Christensen & G. Sigurdsson: *Development of Applicable methods for Evaluating the Safety of Offshore Structures, Part 2.* ISSN 0105-7421 R8504.

PAPER NO. 12: P. Thoft-Christensen & J. D. Sørensen: *A Bibliographical Survey of Structural Reliability.* 2nd edition. ISSN 0105-7421 R8505.

PAPER NO. 13: J. D. Sørensen & P. Thoft-Christensen: *Structural Optimization with Reliability Constraints.* ISSN 0105-7421 R8507.

PAPER NO. 14: M. H. Faber & P. Thoft-Christensen: *Reliability Analysis of a Plane Lattice Structure with Local Imperfections.* ISSN 0105-7421 R8512.

PAPER NO. 15: P. Thoft-Christensen: *Reliability Modelling of Structural Systems.* ISSN 0105-7421 R8514.

PAPER NO. 16: J. D. Sørensen & P. Thoft-Christensen: *Reliability of Tubular Joints, Part 1.* ISSN 0105-7421 R8601.

PAPER NO. 17: P. Thoft-Christensen, G. Sigurdsson & J. D. Sørensen: *Development of Applicable Methods for Evaluating the Safety of Offshore Structures, Part 3.* ISSN 0105-7421 R8604.

PAPER NO. 18: J. D. Sørensen: *Reliability-Based Optimization of Structural Elements.* ISSN 0105-7421 R8608.

PAPER NO. 19: P. Thoft-Christensen: *Recent Advances in Structural Systems Reliability Theory.* ISSN 0105-7421 R8616.

PAPER NO. 20: Wieslaw Paczkowski: *Strain Softening Elements in the β-Unzipping Method.* ISSN 0105-7421 R8617.

(to be continued)

INSTITUTE OF BUILDING TECHNOLOGY AND STRUCTURAL ENGINEERING
THE UNIVERSITY OF AALBORG
SOHNGAARDSHOLMSVEJ 57, DK-9000 AALBORG
TELEPHONE: Int. + 45 - 8 - 14 23 33

STRUCTURAL RELIABILITY THEORY SERIES

PAPER NO. 21: S. R. K. Nielsen & J. D. Sørensen: *Approximations to the Probability of Failure in Random Vibration by Integral Equation Methods.* ISSN 0105-7421 R 8618.

PAPER NO. 22: P. Thoft-Christensen & J. D. Sørensen: *Optimal Strategy for Inspection and Repair of Structural Systems.* ISSN 0105-7421 R 8619.

PAPER NO. 23: P. Thoft-Christensen & J. D. Sørensen: *Reliability Analysis of Tubular Joints in Offshore Structures.* ISSN 0105-7421 R 8620.

PAPER NO. 24: G. Sigurdsson: *Development of Applicable Methods for Evaluating the Safety of Offshore Structures, Part 4.* ISSN 0105-7421 R 8701.

PAPER NO. 25: M. H. Faber & P. Thoft-Christensen: *Instability and Buckling Failure Elements for Columns.* ISSN 0105-7421 R 8702.

PAPER NO. 26: P. Thoft-Christensen & M. H. Faber: *Deflection and Global Instability Failure Elements for Geometrical Non-Linear Structures.* ISSN 0902-7513 R 8706.

PAPER NO. 27: K. J. Mørk, P. Thoft-Christensen & S. R. K. Nielsen: *Simulation Studies of Joint Response Statistics for a One-Degree-of-Freedom Elasto-Plastic Structure.* ISSN 0902-7513 R 8707.

PAPER NO. 28: P. Thoft-Christensen, S. R. K. Nielsen & K. J. Mørk: *Simulation Studies of Joint Response Statistics for Two-Storey Hysteretic Frame Structures.* ISSN 0902-7513 R 8708.

PAPER NO. 29: J. D. Sørensen & P. Thoft-Christensen: *Integrated Reliability-Based Optimal Design of Structures.* ISSN 0902-R 8709.

PAPER NO. 30: S. R. K. Nielsen, K. J. Mørk & P. Thoft-Christensen: *Reliability Analysis of Hysteretic Multi-Storey Frames under Random Excitation.* ISSN 0902-7513 R8711.

PAPER NO. 31: J. D. Sørensen & Rune Brincker: *Simulation of Stochastic Loads for Fatigue Experiments.* ISSN 0902-7513 R8717.

PAPER NO. 32: J. D. Sørensen: *Reliability-Based Optimization of Structural Systems.* ISSN 0902-7513 R8718.

PAPER NO. 33: P. Thoft-Christensen: *Application of Optimization Methods in Structural Systems Reliability Theory.* ISSN 0902-7513 R8719.

PAPER NO. 34: P. Thoft-Christensen: *Recent Advances in the Application of Structural Systems Reliability Methods.* ISSN 0902-7513 R8721.

PAPER NO. 35: P. Thoft-Christensen: *Applications of Structural Systems Reliability Theory in Offshore Engineering. State-of-the-Art.* ISSN 0904-7513 R8722.

INSTITUTE OF BUILDING TECHNOLOGY AND STRUCTURAL ENGINEERING
THE UNIVERSITY OF AALBORG
SOHNGAARDSHOLMSVEJ 57, DK-9000 AALBORG
TELEPHONE: Int. + 45 - 8 - 14 23 33